CFD ANALYSIS OF VENTILATION SYSTEMS FOR GAS TURBINE ENCLOSURES

Alessandro CORSINI[1], Giovanni DELIBRA[1], Stefano MINOTTI[2], Stefano ROSSIN[2]

[1] *Dipartimento di Ingegneria Meccanica e Aerospaziale, Sapienza University of Rome, Via Eudossiana 18, Rome, Italy*

[2] *GE Oil and Gas, Via F. Matteucci, Florence, Italy*

SUMMARY

The fans performance are assessed in configurations according, traditionally, to international standards such as ISO-5801. Similar reference to the so-called standardised airways is used in the design process of industrial fans which provide the ISO test-bench. In recent years, the objective of fan optimization has, in most cases, been re-focused on the optimization of the fan-system coupling in a view to solve for the dynamics of such coupling (either mechanically or aerodynamically). This has been true when ventilating systems are equipped with components such as bended inlets, spinner cones, gravity dampers, that could be responsible for influencing the fan aerodynamic response.

In all these cases, when using CFD, accounting for a real fan geometry inside the domain would be extremely expensive from a computational point of view and too slow for industrial purposes.

When the objective under investigation is the whole ventilation system, it is necessary to account for the single components by means of synthetized methodologies. In particular, fans can be accounted for by simple pressure rise or actuator disks that synthetize their aerodynamic response in the systems of ducting by means of body forces inside the momentum equation.

In the paper the methodology is briefly presented and applied to resolve the fluid-dynamics behaviour of two gas turbine ventilation systems.

INTRODUCTION

Gas turbine enclosures entail a number of components and are considered part of the safety equipment, certified to work in safety for at least 10 years. The purpose of the enclosure is to confine the gas turbine in order to better manage the criticalities arising from operations such as the high temperature and noise and to isolate the gas turbine from the external environment. Finally the enclosure allows to control the risk of explosion and also to control possible fire events. To perform all these tasks the enclosure entails ancillary systems for fire protection, ventilation and others.

Here we focus on the ventilation system, that usually includes, as depicted in Figure 1:

1. a filter house;
2. two identical systems with an axial or a centrifugal fan, a gravity damper and a fire shutter, one to be used in normal operations, the other to work as backup during maintenance or failure. The gravity dampers inside the two ducts opens when the fans are switched on and in so doing ensure that when the backup fan is switched off fluid dynamic short-circuit from primary to secondary fan duct is not possible. Fire shutter are electro-mechanically operated in event of fire.
3. The ducting that connects all the devices and discharge air inside the turbine enclosure;

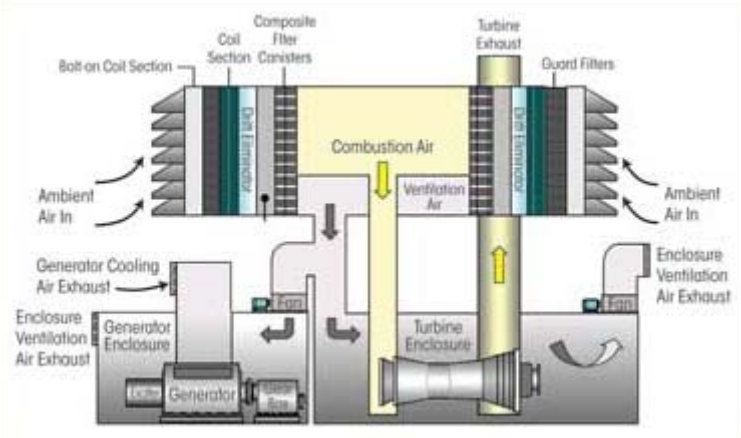

Figure 1: Schematic of the air path in a heavy-duty gas turbine [1].

The ventilation fan needs to be able to adjust to different operating conditions, as, for example, filters get clogged over time or the counter pressure at discharge changes for different reasons. Moreover the same gas turbine can be fitted to different layouts to comply with installation requirements. In this case layout is adjusted with minor or major variations and it is important to ensure that the axial fan is able to operate safely. In this scenario it is important to ensure to avoid designing ventilation system layouts that could accidentally trigger unsteady phenomena that could augment the level of vibrations onto the fan.

Taking a lead from these considerations, a methodology for investigating the robustness of a ventilation system layout for gas turbine enclosure was developed, based on Computational Fluid Dynamics (CFD).

Turbomachinery design, optimization and verification commonly rely on CFD for single devices such as fans or pumps, but the computational costs associated with meshing the details of all the single components of an entire ventilation system are still too high for industrial design. However, when the aim of the numerical investigation is to give insights in the fluid dynamics of the ventilation system and the robustness of its layout to minor or major modifications necessary to adjust to different installations, it is possible to synthetize the effects of the single components.

Here we present a methodology based in synthetic modelling of the principal components of the ventilation system within a CFD framework. The rationale was that of modeling the momentum exchange between fluid and device through source terms into the momentum equation [2].

In the following a brief description is given for each major device of the ventilation system:

- filters;
- fan;
- gravity damper and fire shutter.

Results were validated against two different layouts of ventilation systems for the same gas turbine enclosure.

FILTER MODELLING

Filters inside the filter house were modelled as a porous medium, introducing into momentum equation a pressure gradient calculated according to Darcy-Forchheimer Law [3]:

$$\nabla p = -\frac{\mu \vec{V}}{K} - \rho\beta|V|\vec{V} \tag{1}$$

where ∇p is the pressure gradient, μ the dynamic viscosity of the fluid, ρ the density of the fluid and K and β two experimental coefficients depending on the properties of the porous material. The main issue of this approach is that each material has a specific value for the K and β coefficients, that according to Bejan [3] vary over a range of three orders of magnitude from one material to the other. Moreover these coefficients can only be measured experimentally with a long and expensive procedure, so that usually they are not available for filters on the market. This lead to the necessity to derive them through a regression technique based on the available values of pressure drop versus flow rate curves in data sheets. The vectorial form of equation (1) allowed also to account for the directionality of the filters.

MODELLING OF GRAVITY DAMPER AND FIRE SHUTTER

The gravity damper was modelled as a body force inside the momentum equation. In this case the characteristic curve of the gravity damper was given in terms of pressure drop vs mass flow rate and was correlated with the angle of inclination of the fins with the relationship given in [4]:

$$\nabla p = \left(0.35 \cdot 10^{0.0323\delta}\right) \cdot \frac{1}{2}\rho V_{in}^2 \tag{2}$$

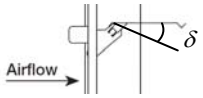

This allowed to align the pressure drop with the inclination of the fins δ. Finally, the fire shutter was modelled as a fully open gravity damper (i.e. $\delta = 0°$).

MODELLING OF THE FAN

The fan is the most complex device in the system and was modelled in order to accurately reproduce its performance over the whole operating range of the fan. Different methodologies were proposed in open literature [5], here we focus on a new actuator disk and line methodology to simulate the presence of an axial fan, and a pressure discontinuity to account for the presence of a gravity damper. This methodology is able to account for radial flows in the actuator disk and, if run in unsteady mode, to include the effect of rotation of the fan, as well as the real number of blades, with a modification similar to the one assessed in Sorensen and Shen [6] for wind turbines actuator disks.

Here the fan was modeled by adding to the momentum equations the body forces corresponding to the interaction with the flow. Those were determined by means of quasi 3D viscous calculations based on the discretization of the blade into 10 2D blade sections. For each airfoil the lift and drag curves against the angle of attack are computed. The model of the fan then was able to compute axial, tangential and radial components of the force exerted by the rotor and add them to the flow field and in this way to correctly adjust to the whole operating range of the fan with great accuracy.

All the equations of each model will be given and explained in the final manuscript due to space limitations. The models were validated against experimental data coming from fan charts and empirical correlations [7] and are here used to predict and analyze the flow field inside two real-geometry ventilation systems for gas turbine enclosure. Flow field was analyzed at different flow

rates to assess the robustness of the layout and how the different arrangement reflects onto the fan operations.

NUMERICAL METHODOLOGY AND SETUP

The Reynolds-Averaged incompressible Navier-Stokes equations were solved using OpenFOAM 2.3.x [8], an open-source software for computational fluid dynamics. The synthetic models of the fan, filters and gravity dumper were implemented inside the standard library in order to simulate the presence of the fan, and coupled with a standard high-Reynolds implementation of the k-ε model. This assuming that integration to the wall with low-Reynolds approach would not be necessary with this kind of synthetic description of the fan.

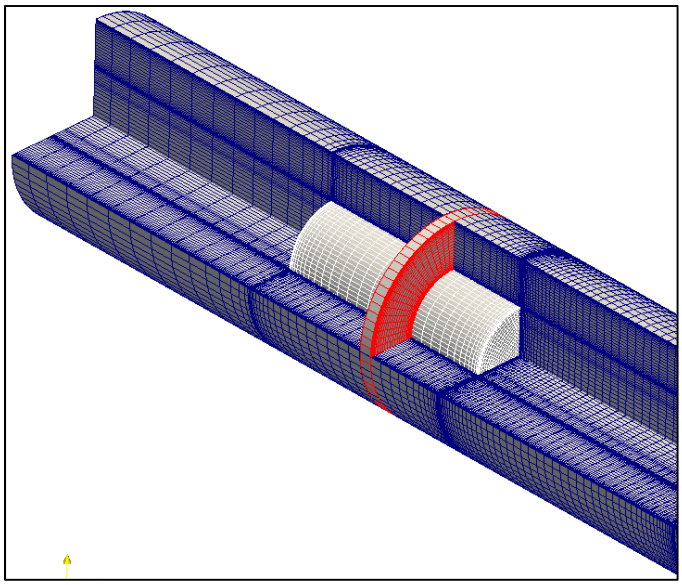

Figure 2: Overview of the computational domain near the hub of the fan – only ¾ of the azimuth of the duct are shown. Detailed view of the ADM region.

The linearised system of equations was solved using a GAMG solver for pressure and smoothSolver for the other quantities. Tolerance for convergence of the solvers was set to 10^{-7}. The convection terms of the transport equations were discretized using QUICK scheme. The test rig was initialised with the ADM switched off for 3000 iterations. Final results were gathered after another 7000 iterations with the ADM switched on. In the following the two different geometries are labeled as G_1 and G_2. Both geometries were investigated at 4 different flow rates, Q_1 to Q_4, Table 1.

.Table 1 - Operating conditions investigated

Operating conditions
$Q_1 = 23.2\ m^3/s$
$Q_2 = 20.0\ m^3/s$
$Q_3 = 17.7\ m^3/s$
$Q_4 = 15.0\ m^3/s$

Computations were run in steady-state mode with RANS approach for all the flow rates.

RESULTS

G1 configuration

In the following results for RANS computations of the *G1* configuration at Q_1, and Q_4 are illustrated. First, Figure 3 provides an overview of the velocity field inside the filter chamber. Specifically, the 3D streamlines and the distribution of the computed turbulent kinetic energy are used to show the behaviour of the ventilation system as per the coupling of the synthetic models for the filter, the fan and the fire shutter. Notably, the position of the duct relative to the filter introduces a large inflow distortion and results in a non-uniform distribution at the entrance of the active fan duct.

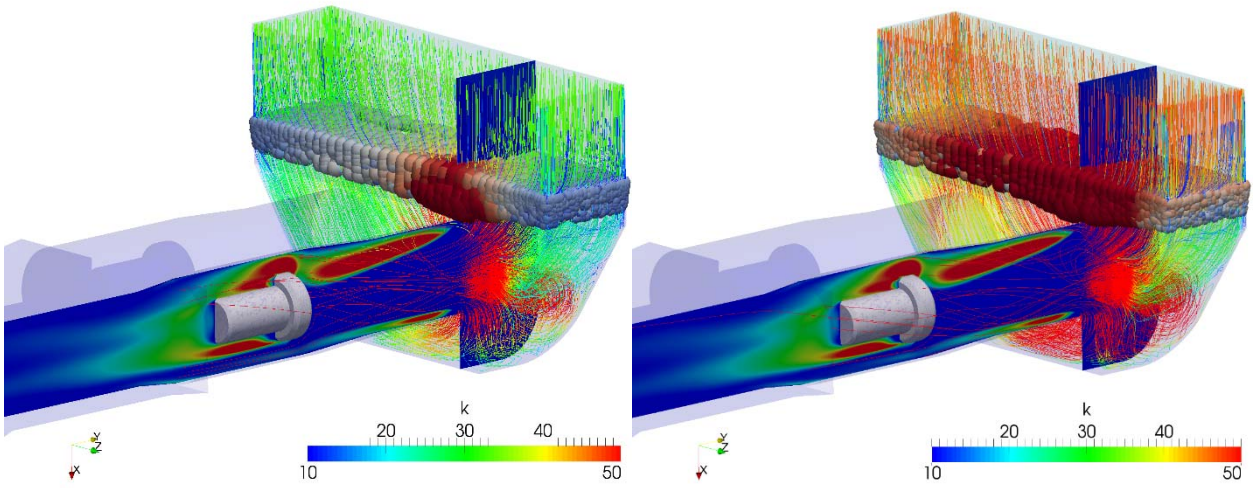

Figure 3 – Overview of 3D streamlines in the filter chamber and distribution of k onto an axial section in the active fan duct. G1, Q1 (left); G1 Q4 (right). Sphere glyphs show the pressure drop in the porous medium.

Figure 3 also shows the presence of a slow re-circulating motion in the plenum upstream and a separation is noticeable at the entrance of the fan.

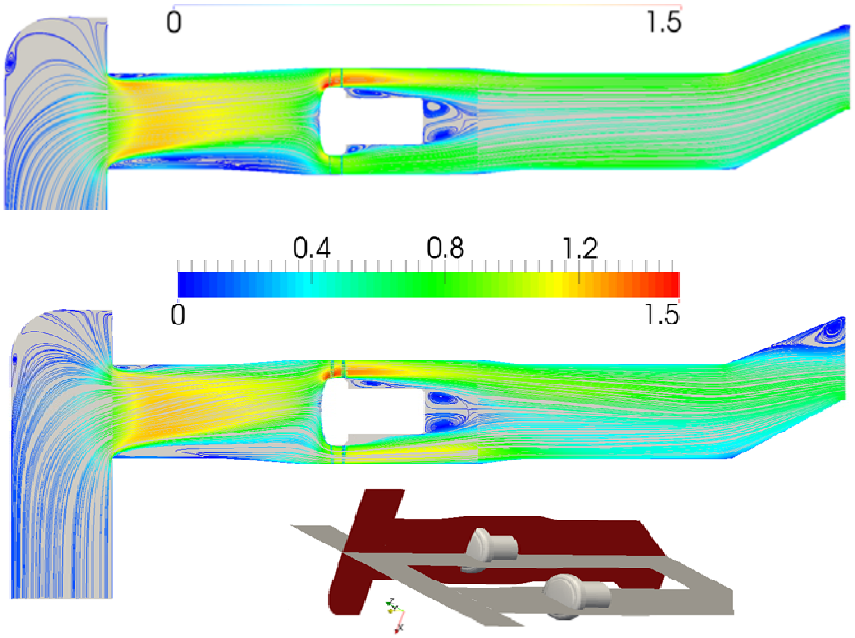

Figure 4 – Overview of 2D streamlines colored with normalised velocity magnitude on the plane highlighted in red in the sketch. G1 Q (top); G1 Q4 (bottom). Velocity values in colors account only for the parallel-to-the-plane component of velocity

Figure 4 provides further insight of the development of secondary motions inside the active fan ducts, and highlights how most of the velocity defect is lost when entering the fan section. There are however differences moving from the higher to the lower flow rate, due to the development along the duct of the streamwise extension of the separation upstream of the fan.

G2 configuration

In the following results for RANS computations of the *G2* configuration at Q_1, and Q_4 are illustrated. In Figure 5, an overview of the velocity field inside the filter chamber is given using the 3D streamlines and the distribution of the computed turbulent kinetic energy. It is confirmed that the porous media, used to model the filter, features a non-uniform pressure drop due to the relative location of the active duct to the plenum. This circumstance results into the presence of a large region of recirculation which is ironed out in the vicinity of the duct entrance. Here a separation is visible at the junction of the duct with the filter house.

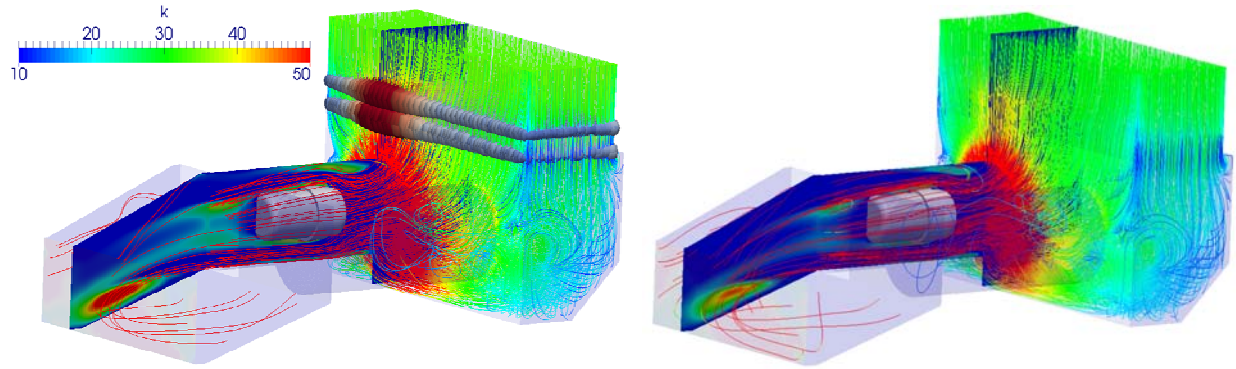

Figure 5 – Overview of 3D streamlines in the filter chamber and distribution of k onto an axial section in the active fan duct. G2, Q1 (left); G2 Q4 (right). Sphere glyphs show the pressure drop in the porous medium.

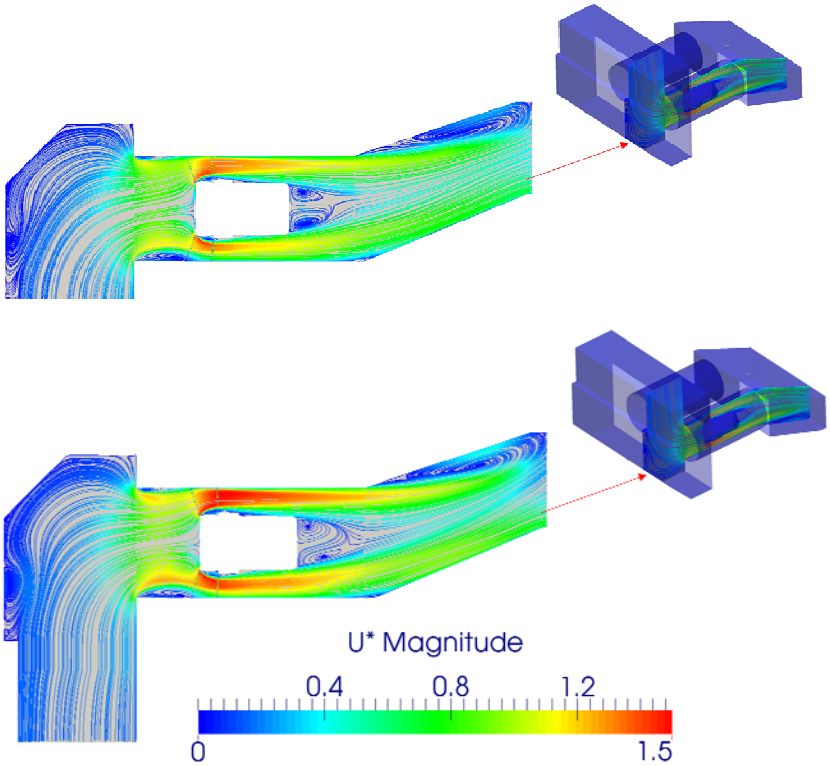

Figure 6 – Overview of 2D streamlines colored with normalised velocity magnitude on the plane highlighted in the sketch. G2 Q1 (top); G2 Q4 (bottom). Velocity values in colors account only for the parallel-to-the-plane component of velocity

Figure 6, then, illustrates the development of secondary motions entering the active fan ducts. Notably, it is found that the small separations are strained by the fan irrespective of the operating conditions.

CONCLUSIONS

The comparative analysis of the two configurations highlighted that:

1. G1 configuration was able to operate at all the flow rates working in similarity conditions. In other words at all the flow rates the fan was fed with the same velocity profile, Figure 7. On the contrary the G2 configuration did not show the same trend at the higher flow rate Q1, Figure 8. This was related to the different shape of the filter house and was confirmed by an additional investigation of the G1 layout combined with the G2 filter house.

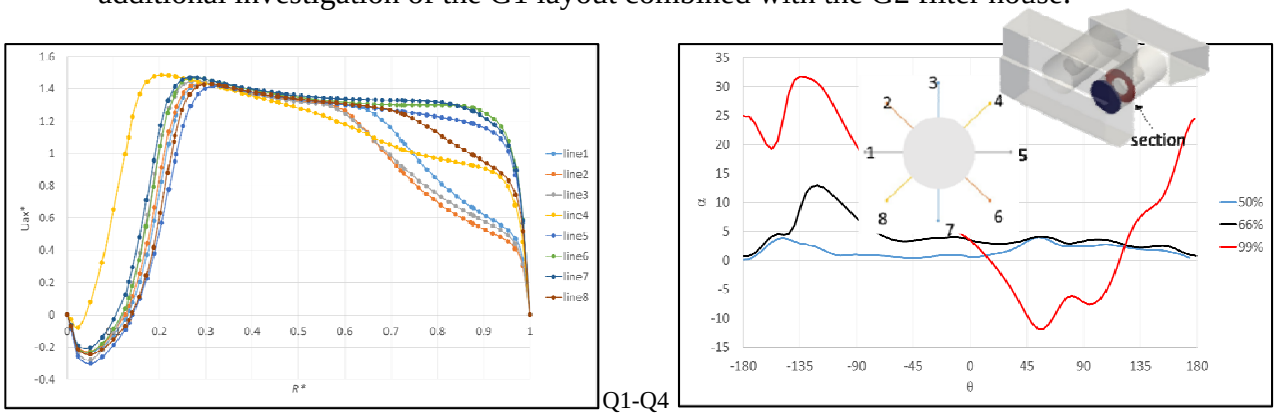

Figure 7. G1 configuration, Q1 to Q4. Left: spanwise axial velocity profiles normalised with bulk velocity at the fan inflow along 8 lines (see insert). Right: azimuthal variation of angle of attack @ 50%, 66% and 99% of the rotor span.

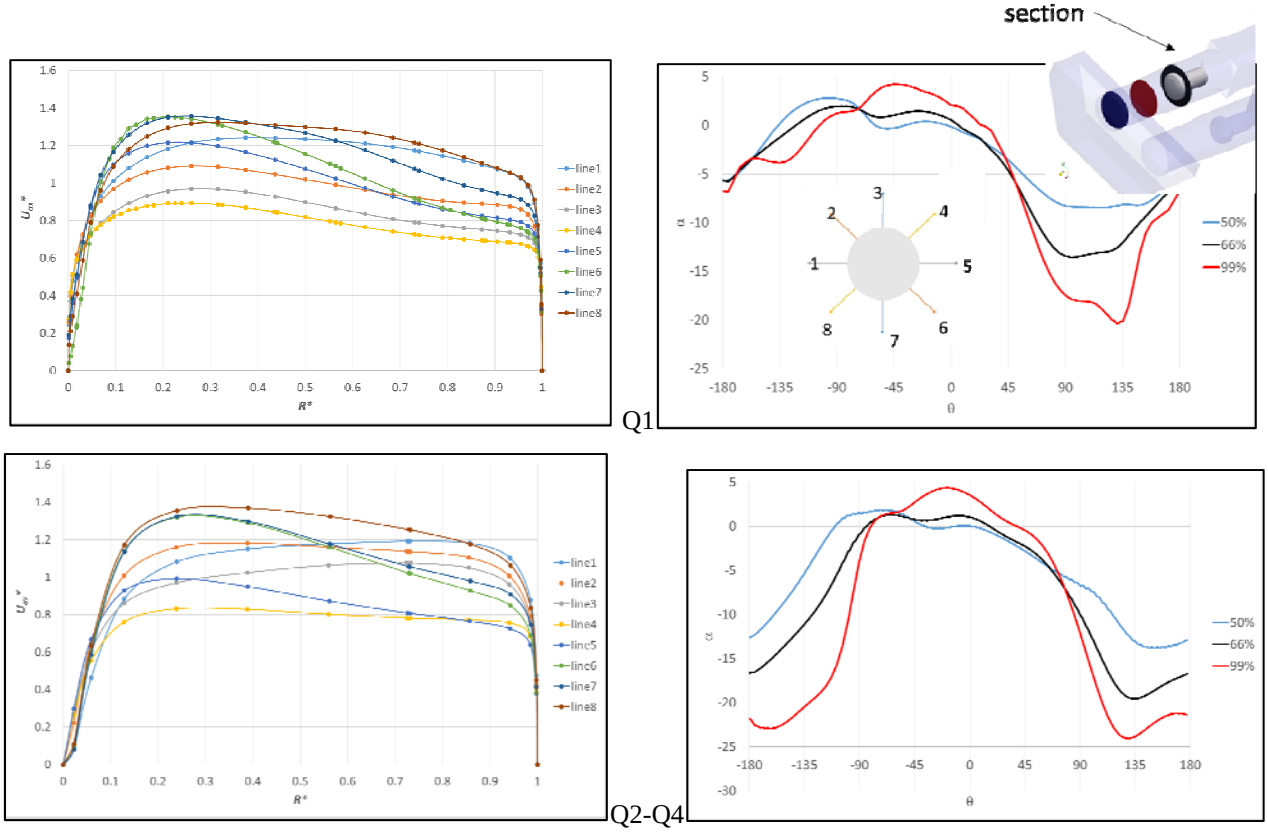

Figure 8. G2 configuration, Q1 (top row), Q2 to Q4 (bottom row). Left: spanwise axial velocity profiles normalised with bulk velocity at the fan inflow along 8 lines (see insert). Right: azimuthal variation of angle of attack at 50%, 66% and 99% of the rotor span.

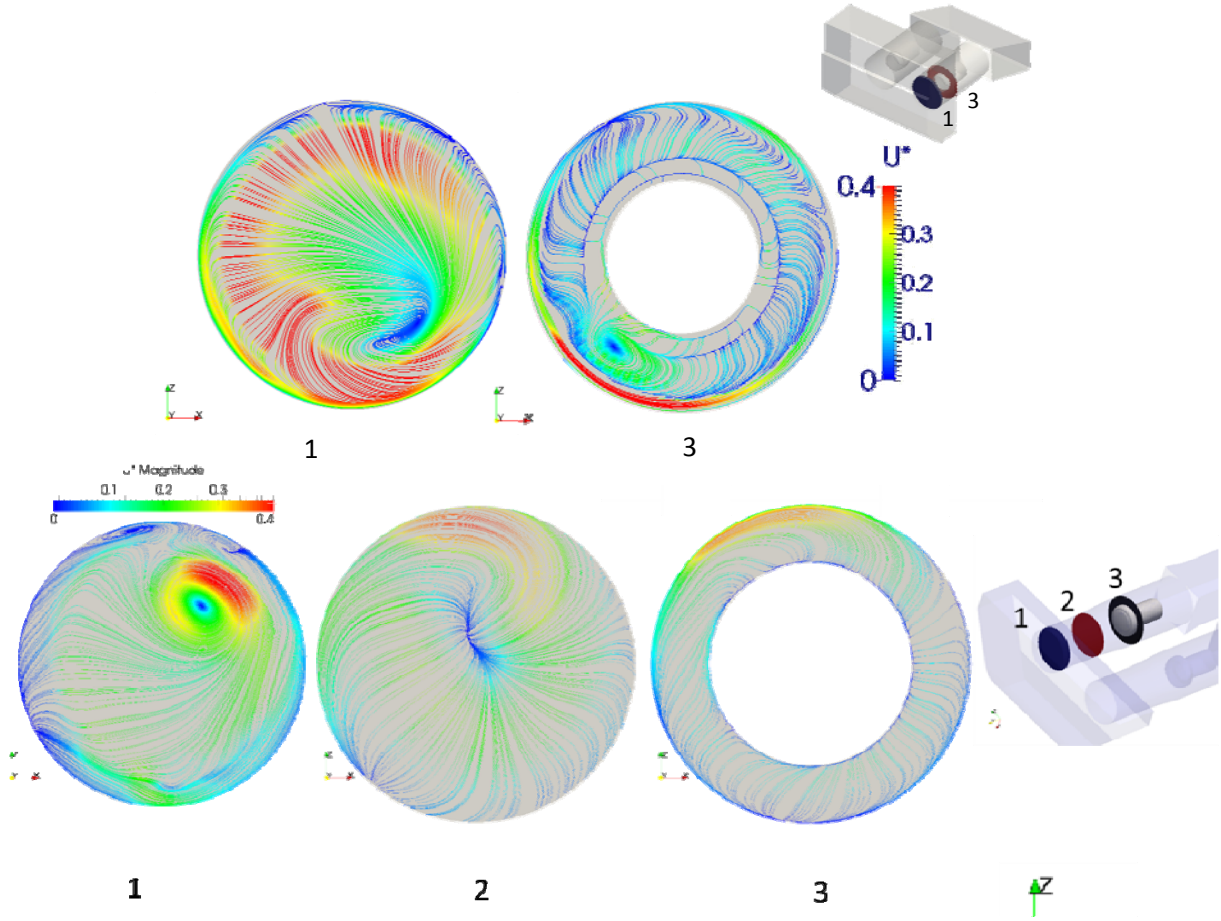

Figure 9. Overview of 2D streamlines colored with normalised swirl velocity magnitude on the planes highlighted in the sketch. Top: G1 at Q1. Bottom: G2 at Q1.
Velocity values in colors account only for the parallel-to-the-plane component of velocity.

REFERENCES

[1] Di Campli, J., Pan, J., and Arsenault, M. - *Gas turbine air filter system optimization*. Power Engineering, (1), **2015**.

[2] Kundu, P., K., Cohen, I. M., and Dowling, D., R. - *Fluid Mechanics, Fifth Edition*. Academic Press, **2011**.

[3] Bejan, A. - *Convection Heat Transfer*. Wiley, **2013**.

[4] Idelchik, I., E. - *Handbook of Hydraulic Resistance*. Jaico Publishing House, **2005**.

[5] van der Spuy, J., S., von Backström, T., W., Kröger, D., G. - *Performance of low noise fans in power plant air cooled steam condensers*. Noise Control Engineering Journal, Volume 57, Number 4, pp. 341-347, **2009**.

[6] Sorensen, J., N., Shen, W., Z. - *Numerical Modeling of Wind Turbine Wakes*. J. Fluids Eng. 124(2), pp.393-399, **2002**.

[7] Corsini, A., Delibra, G., Minotti, S., and Rossin, S.- *Numerical assessment of fan-ducting coupling for gas turbine ventilation systems*, ASME paper GT2015-42449, Turbo Expo 2015, Montreal, Canada, **2015**.

[8] Weller, H.G., Tabor, G., Jasak, H., & Fureby, C. - *A Tensorial Approach to Continuum Mechanics using Object-oriented Techniques*. Journal of Computational Physics, vol. 12(6), pp. 620–631, **1998**.